Monatshefte für Chemie 124, 493–509 (1993)

Monatshefte für Chemie
Chemical Monthly

Redox Kinetics of Metal Complexes in Nonaqueous Solutions: Oxidation of a Series of Tris(1,10-phenanthroline)iron(II) Ions by Hexakis(trimethylphosphate)iron(III) in Acetonitrile – A Reactivity-Selectivity Relationship

R. Schmid*, **Liang-feng Han**, **K. Kirchner**, and **V. N. Sapunov****

Institut für Anorganische Chemie, Technische Universität Wien, A-1060 Wien, Austria

Summary. The kinetics of outer-sphere oxidation of $Fe(Xphen)_3^{2+}$ ions ($X = H$ or several methyl substituents) in acetonitrile (*Me*CN) solution by iron(III), introduced as $Fe(tmp)_6(ClO_4)_3$ (*tmp* = trimethylphosphate), have been investigated at 25 °C. The reactions are very complex because of solvation equilibria between *tmp* and *Me*CN coordinated at Fe^{3+}, with a reduction potential difference of 0.20 V for the replacement of one *tmp* by *Me*CN. This makes the various solvate species highly different in driving force. The second essential feature is the high charge-type of $+2/+3$. This brings about strong acceleration by salt because of ion association reducing the work necessary to overcome the Coulombic repulsion in forming the precursor complex.

The task was to deconvolute two kinds of speciation: the ionic and the solvate speciations. The analysis suggests the concurrent existence of five $Fe(tmp)_n^{3+}$ ($n = 2$–6) species among which four species ($n = 2$–5) are reacting, with an additional mono and bis perchlorate ion pair for each n. Extra complications arise as some of the solvation equilibria are not always fast compared to the redox reactions, leading to non-first order rate constants.

Although the rate constants could not be defined with the desired precision, at least two results are worth noting: (i) The relative effects of driving force and charge are highlighted in controlling overall reactivity. (ii) The stronger the reducing power of the $Fe(Xphen)_3^{2+}$ moiety, the less it can distinguish between the various solvate species (reactivity-selectivity relationship).

Keywords. Nonaqueous electron transfer; Iron(III)trimethylphosphate complexes; Ligand exchange.

Redox-Kinetik von Metallkomplexe in nicht-wäßrigen Lösungsmitteln: Oxidation einer Serie von Tris(1,10-phenanthrolin)eisen(II)-Ionen mit Hexakis(trimethylphosphat)eisen(III) in Acetonitril-eine Reaktivitäts-Selektivitäts-Beziehung

Zusammenfassung. Es wurde die Kinetik der Outer-sphere Oxidation einer Reihe von $Fe(Xphen)_3^{2+}$ Ionen ($X = H$ oder verschiedene Methylsubstituenten) mit Eisen(III), eingeführt als $Fe(tmp)_6(ClO_4)_3$

** Permanent address: Chemical Technological Mendeleev Institute, Miuskaja 9, 125820 Moscow, Russia.

(*tmp* = Trimethylphosphat), bei 25 °C in Acetonitril (*Me*CN) untersucht. Diese Reaktionen sind sehr komplex, da gebundenes *tmp* teilweise durch *Me*CN ausgetauscht wird, wobei der Ersatz eines *tmp*-Moleküls durch *Me*CN das Redoxpotential um 0.2 V verschiebt. Deshalb sind die verschiedenen Solvatkomplexe in ihrer Reaktivität sehr unterschiedlich. Ein zweites wesentliches Merkmal der untersuchten Reaktionen ist der hohe Ladungstyp von +2/+3. Das bringt eine starke Erhöhung der Reaktionsgeschwindigkeit durch Elektrolytzusatz infolge von Ionenassoziation mit sich, die die Coulombsche Arbeit für die Bildung des Precursorkomplexes reduziert. Die Aufgabe bestand demnach in der Aufklärung von zwei Speziationsarten, der Solvations- und Ionenassoziationsgleichgewichte. Die Analyse weist auf das gleichzeitige Vorliegen von fünf $Fe(tmp)_n^{3+}$ Species ($n = 2$–6) hin, wobei vier von ihnen ($n = 2$–5) reagieren. Zusätzlich gibt es für jedes n noch Ionenpaare und Ionentriplets mit Perchlorat. Eine zusätzliche Komplizierung ergibt sich, weil bestimmte Solvationsgleichgewichte nicht immer schnell sind im Vergleich zu den Redoxreaktionen, die dann nicht mehr pseudo-erster-Ordnung sind.

Wenn auch die Geschwindigkeitskonstanten nicht mit der üblicherweise gewünschten Präzision angegeben werden können, sind zumindest zwei Ergebnisse nennenswert: (a) Es wird die relative Bedeutung der driving force und der Reaktantenladung für die Gesamtreaktivität hervorgehoben und (b) Je stärker die Reduktionskraft des $Fe(Xphen)_3^{2+}$ Ions, desto weniger kann es die verschiedenen Solvatspezies unterscheiden (Reaktivitäts-Selektivitäts-Beziehung).

Introduction

Studies of electron transfer reactions between metal complexes in nonaqueous solutions have received considerable attention in the last few years due to their fundamental role in chemical processes. The majority of these studies were done on outer-sphere systems involving substitution inert reactants with low or zero charges, to eliminate or at least minimize, ion pair and ionic strength effects.

We decided to enlarge the scope by the inclusion of substitutionally labile reactants [1, 2]. In the previous report [2] we characterized the oxidations of methyl-substituted tris(1,10-phenanthroline)iron(II) ions by iron(III), introduced as $Fe(dmf)_6(ClO_4)_3$, in acetonitrile. The redox-active species were found to be $Fe(dmf)_3(MeCN)_3^{3+}$ and $Fe(dmf)_4(MeCN)_2^{3+}$. Both solvation equilibrium constants and redox rate constants could be determined.

These studies also showed that one can utilize the redox process as an indicator for solvent replacement reactions and for the characterization of $Fe(solvent)_6^{3+/2+}$ complexes in solution. Thus, the study of such reactions may prove to be a useful approach better to understand the relative solvent power of mixed solvents.

As part of our ongoing effort in this regard we use in the present work the trimethylphosphate (*tmp*) analogue, $Fe(tmp)_6(ClO_4)_3$, as oxidizing agent to learn how the kinetic and thermodynamic parameters are changed because of the lower Lewis basicity of *tmp* compared to *dmf*, as indicated by the Gutmann donor numbers [3].

Experimental Part

The tris 1,10-phenanthroline complexes of iron(II) perchlorate, $Fe(X\text{-}phen)_3^{2+}$, with X = H, 5,6-Me_2, 4,7-Me_2, 3,4,7,8-Me_4 (= Me_4), and 3,4,5,6,7,8-Me_6 (= Me_6) have been made as before [2]. Hexakis(trimethylphosphate)iron(III) perchlorate was made in the same manner as the *dmf* analogue [2]. *Perchlorate salts of metal complexes with organic ligands are potentially explosive. Therefore, the drying temperature was kept below 50 °C, and the solid compounds have been handled with great caution.*

Trimethylphosphate (Merck) was purified by refluxing over calcium hydride for several hours and distilled under nitrogen. The electrolyte $Bu_4N(ClO_4)$ was prepared as before [1]. The kinetics were measured at 25 °C on a Durrum D-110 stopped-flow spectrometer as before by following the consumption of the ferroin reactant [2]. All of the kinetic measurements were made with the oxidant taken in at least tenfold excess over the concentration of the phenanthroline complexes. The latter was always 0.1 m*M*. The cyclic voltammetric measurements of $Fe(tmp)_6(ClO_4)_3$ in *tmp* were carried out at 25 °C as before [2]. The ^1H NMR experiments were performed on an IBM NR300 instrument operating at 300 MHz at 20 (+/−1) °C. The temperature readings were calibrated against the temperature dependence of the proton chemical shifts of acidified methanol (0.5% HCl).

Results

Experimental reaction rates were found to increase in the order of substituents $H < 5,6\text{-}Me_2 < 4,7\text{-}Me_2 < Me_4 < Me_6$ by about a factor of 50 overall, and this is the order of the redox potentials (Table 1). The rates decreased when extra *tmp* (termed $[tmp]_0$ or $[L]_0$ in the following) was added, and the rates increased, when salt (Bu_4NClO_4) was added. All reactions investigated in this work were quantitative as determined from the absorbance changes. Thus, all five systems could be analyzed under a large variety of conditions with regard to the concentration of Fe(III), extra added electrolyte, and extra added *tmp*, such that the observed rates vary by as much as 2–3 orders of magnitude in each system.

Oxidations of $Fe(phen)_3^{2+}$, $Fe(5,6\text{-}Me_2phen)_3^{2+}$ *and* $Fe(4,7\text{-}Me_2phen)_3^{2+}$

All experiments with no extra added *tmp* exhibited non-linear log (Absorbance) vs.

Table 1. Redox potentials[a] for $Fe^{3+/2+}$ in acetonitrile at 25 °C

Complex	$E_{1/2}$[b], V	Refs.
$Fe(tmp)_6^{3+/2+}$	1.34_8	this work[c]
$Fe(Me_6phen)_3^{3+/2+}$	1.52_0	[2]
$Fe(tmp)_5(MeCN)^{3+/2+}$	1.55	[d]
$Fe(3,4,7,8\text{-}Me_4phen)_3^{3+/2+}$	1.57_5	[2]
$Fe(4,7\text{-}Me_2phen)_3^{3+/2+}$	1.66_7	[2]
$Fe(tmp)_4(MeCN)_2^{3+/2+}$	1.75	[d]
$Fe(5,6\text{-}Me_2phen)_3^{3+/2+}$	1.77	[2]
$Fe(phen)_3^{3+/2+}$	1.83_6	[1]
$Fe(tmp)_3(MeCN)_3^{3+/2+}$	1.95	[d]
$Fe(tmp)_2(MeCN)_4^{3+/2+}$	2.16	[d]
$Fe(MeCN)_6^{3+/2+}$	2.56_4	[1]

[a] The potentials are referenced to BCr (−1.118 V vs. ferrocene/ferricenium)

[b] $E_{1/2}$ taken as $(E_P^{red} + E_P^{ox})/2$

[c] Measured in *tmp*; scan rate = 100 mV/s, 0.1 *M* $Bu_4N(PF_6)$ was present, reactant concentration ca. 1 m*M*

[d] Interpolated on the crude assumption that the reduction potential is a linear function of the *tmp* and *Me*CN ligands

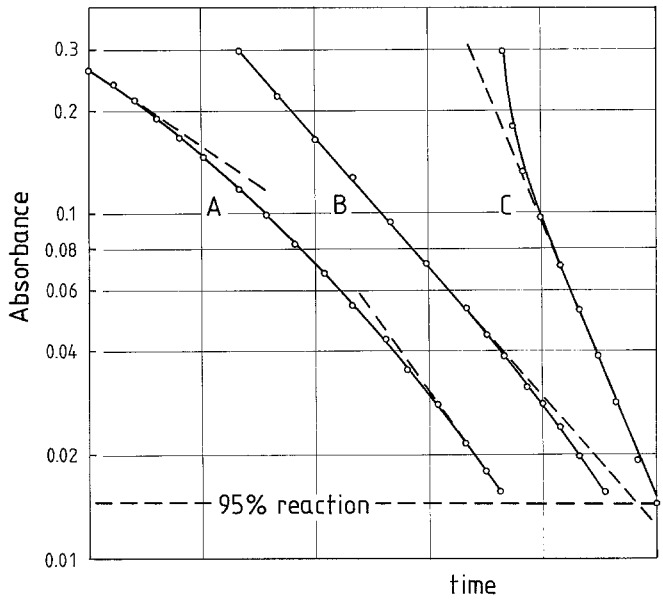

Fig. 1. Typical semilog plots for the oxidation of 0.1 m*M* solutions of various ferroin complexes (time axis in s/div in parentheses): (A) Fe(5,6-$Me_2phen)_3^{2+}$ + 24 m*M* Fe(III) (0.1); (B) Fe($Me_4phen)_3^{2+}$ + 24 m*M* Fe(III) (0.0024); (C) Fe($Me_6phen)_3^{2+}$ + 2 m*M* Fe(III) (0.012). (A) and (B) without added salt, (C) with 190 m*M* Bu_4NClO_4 added

time ($= \log A/t$) plots, the rates increasing during the course of reaction. A typical example is shown in Fig. 1A. Rate constants $k(i)$ obtained from the initial slopes of these plots were used in order to compare the different reaction systems. Values of $k(i)$ were found to increase non-linearly with [Fe(III)] in the absence of extra added electrolyte (see, e.g., Table 4). In contrast, when the variation in perchlorate

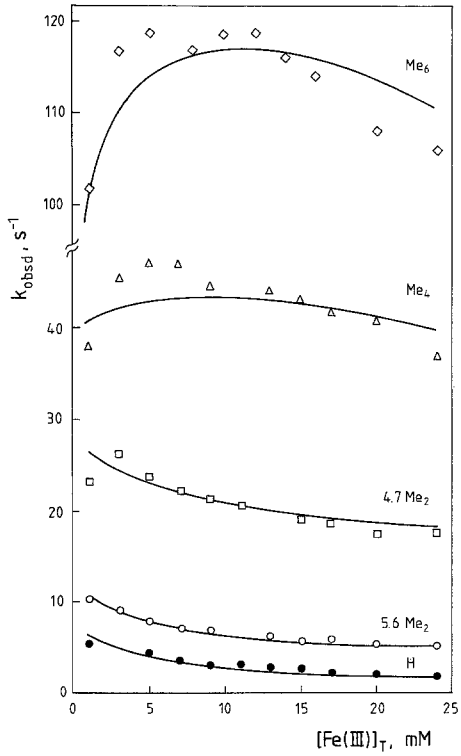

Fig. 2. Variation of observed initial rate constants for the oxidation of various Fe($Xphen)_3^{2+}$ complexes with the total iron(III) concentration at constant perchlorate level. Solid lines are calculated values of $k(i)_{lim}$

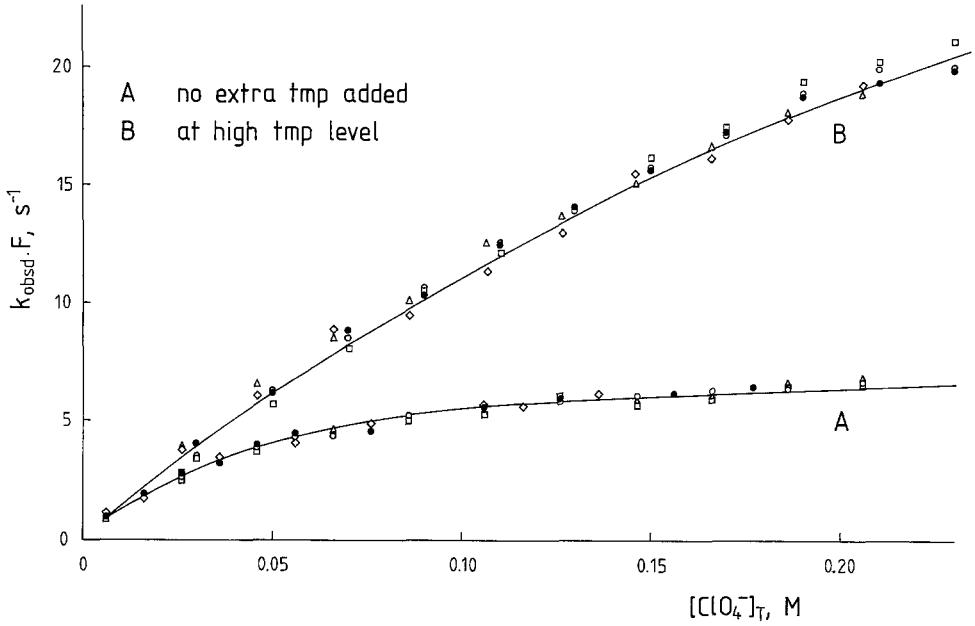

Fig. 3. Dependence of observed rate constants on added Bu_4NClO_4 in terms of the total ClO_4^- concentration from all sources, for all phen complexes investigated with substituents ● H, ○ 5,6-Me_2, □ 4,7-Me_2, △ Me_2, ◇ Me_6. The rate constants are normalized for the no added salt and no extra added *tmp* value for the Fe(*phen*)$_3^{2+}$ reaction to unity. (A) Initial rate constants with no additional *tmp* added, [Fe(III)] = 2 m*M*. The transformation coefficients *F* are as follows: H 0.725; 5,6-Me_2 0.375; 4,7-Me_2 0.152; Me_4 0.074; Me_6 0.044. (B) Pseudo-first-order rate constants at high *tmp* concentration level. Concentrations (m*M*) of iron(III) and additionally added *tmp* with transformation coefficients *F* in parentheses, H 10, 50 (28.5); 5,6-Me_2 10, 50 (10.0); 4,7-Me_2 10, 200 (19.6); Me_4 2, 200 (36.9); Me_6 2, 200 (11.5). The solid lines are calculated from Eq. (10) according to the text. The fit parameters (s^{-1}) of k_A and k_B were for (A) 13.58 and 8.26, and for (B) 18.00 and 39.16, respectively. The line for curve B is for 10 m*M* Fe(III) and differs slightly from that calculated for 2 m*M* Fe(III)

concentration is compensated for by the addition of Bu_4NClO_4, the initial rate constants decrease with increasing [Fe(III)] in the cases of *phen* and 5,6-Me_2*phen*, and pass through a maximum in the 4,7-Me_2*phen* case (Fig. 2). Further, *k*(*i*) increases non-linearly towards saturation upon the addition of Bu_4NClO_4 at fixed [Fe(III)]. The curves for the added salt dependences for the various *phen* complexes can be superimposed onto the other by linear transformation (Fig. 3, lower curve) which simplifies the fitting procedures.

Addition of extra *tmp* slows down the reaction drastically and eventually, as the *tmp* concentration increased, pseudo-first-order kinetics are obtained. The amount of *tmp* needed to produce pseudo-first-order kinetics increases with the reactivity of the ferroin complexes; i.e. H < 5,6-Me_2 < 4,7-Me_2 < Me_4 < Me_6. The decrease of the pseudo-first-order rate constant with [*tmp*] for the Fe(*phen*)$_3^{2+}$ reaction is depicted in Fig. 4. The inset of Fig. 4 shows the same dependence at 0.15 *M* Bu_4NClO_4. Finally, the variation of the pseudo-first-order rate constant with salt concentration has been measured at high [*tmp*]. The curves pertinent to different *phen* complexes are superimposable by linear transformation (upper curve in Fig. 3).

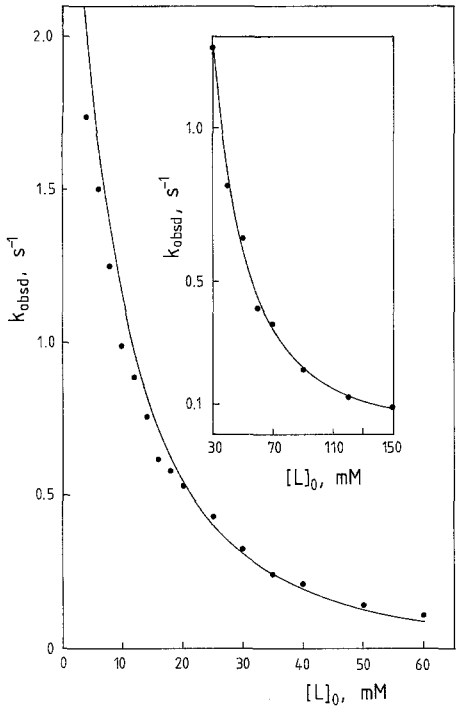

Fig. 4. Dependence of the pseudo-first-order rate constant for the reaction of $Fe(phen)_3^{2+}$ (0.1 m*M*) and Fe(III) (10 m*M*) upon the addition of extra *tmp*. Inset: The same dependence but at 0.15 *M* Bu_4NClO_4. The full lines are calculated according to the text

Oxidations of $Fe(Me_4phen)_3^{2+}$ *and* $Fe(Me_6phen)_3^{2+}$

In the absence of added *tmp*, $\log A/t$ plots are linear in the early stages up to about 80% reaction followed by a rate increase in the final parts (Fig. 1B). The first-order range extended when salt was added (except for high salt concentrations, see below). As in the slower reactions above, values of $k(i)$ increase non-linearly with Fe(III) and salt. When working at a constant $[ClO_4^-]$, the Fe(III) dependence has a maximum (Fig. 2). An additional feature appears in the Me_6phen system where at a high salt level deviations from a first-order rate law occur in the initial stages (Fig. 1C). The salt dependences of the rate constants with and without extra added *tmp* can be included in Fig. 3 by using mapping coefficients.

As before upon addition of *tmp*, apart from a drastic decrease in the rates, first-order behavior is observed. The results of the stopped-flow experiments which had half-lives $<0.5\,s^{-1}$ are dependent on whether *tmp* is added to the oxidant or to the reductant.

Speciation of Fe(III)

As in the preceding studies, the speciation was studied by ^1H NMR spectroscopy [1, 2, 4]. At 20 °C separate resonances of coordinated (in the range of 6–9 ppm) and bulk *tmp* (at about 3.6 ppm) could be detected in the spectrum of $Fe(tmp)_6(ClO_4)_3$ dissolved in CD_3CN. Because of coupling to ^{31}P, the signal of free *tmp* is split into a doublet. The signal of the residual protons of CD_3CN has been used as reference for the shifts. The coordination numbers, n_{tmp}, obtained from the relative areas of the free and coordinated peaks are given in the first row of Table 2 for various

Table 2. Numbers, n_{tmp}, of trimethylphosphate molecules coordinated at iron(III) in solutions of $Fe(tmp)_6(ClO_4)_3$ in *Me*CN

$[Fe(III)]_T$ mM	NMR	n_{tmp} kinetics[a]
3.00	3.90 +/− 0.20	4.07
7.15	4.56 +/− 0.10	4.47
11.13	4.70 +/− 0.15	4.65
30.50	4.89 +/− 0.20	5.03

[a] Calculated from the β values given in Table 3

iron(III) concentrations. The error is greater the higher the iron(III) concentration due to the onset of overlap of coordinated and free ligand signals.

Discussion

In accordance with previous reports on the $Fe(dmf)_6^{3+}$ system, the decrease of rate when extra *tmp* is added is indicative of solvation equilibria between *tmp* and *Me*CN coordinated at Fe^{3+}, with ions of higher *tmp* content being less reactive. Further, since ions with charges as high as 2+ and 3+ are involved in these reactions, ion-pair formation as well as ionic strength effects have to be taken into consideration.

Evaluation of Solvation Equilibria

From the occurrence of non-linear log A/t plots and from the observation that these plots, for the faster systems, in the experiments with extra added *tmp* depend on whether *tmp* was added to the oxidant or to the reductant we conclude that at least one of these equilibria is on the time scale of the redox processes. Only when first-order kinetics are observed at higher [*tmp*], can the solvation equilibria be considered as being established rapidly compared to electron transfer. For the evaluation of the solvation equilibria the *phen* system was used, since there the least amount of *tmp* were necessary to produce first-order kinetics. The variation of pseudo-first-order rate constants, k_{obsd}, with [*tmp*] together with the NMR data requires at least three solvation equilibria to be involved. On the basis of three equilibria, however, much slower initial rates than experimentally found would be anticipated for the reactions run with low iron(III) concentration and without adding extra *tmp*. Therefore four solvation equilibria are suggested (in the following *tmp* is denoted as *L* and coordinated *Me*CN is omitted),

$$FeL_6^{3+} \Leftrightarrow FeL_5^{3+} + L \quad \beta_1 \tag{1}$$

$$FeL_6^{3+} \Leftrightarrow FeL_4^{3+} + 2L \quad \beta_2 \tag{2}$$

$$FeL_6^{3+} \Leftrightarrow FeL_3^{3+} + 3L \quad \beta_3 \tag{3}$$

$$FeL_6^{3+} \Leftrightarrow FeL_2^{3+} + 4L \quad \beta_4 \tag{4}$$

Table 3. Summary of the equilibrium parameters used in the calculations

Parameters	Eq.	Values
β_1, M	(1)	$0.055 +/- 0.02$
β_2, M^2	(2)	$(7 +/- 2) \times 10^{-4}$
β_3, M^3	(3)	$(1 +/- 0.5) \times 10^{-6}$
β_4, M^4	(4)	$(2 +/- 1) \times 10^{-9}$
K_1, M^{-1}	(5)	$70 +/- 20$
K_2, M^{-1}	(6)	$15 +/- 5$
K_3, M^{-1}	(7)	$3 +/- 1$

with all of the species, except for FeL_6^{3+}, being redox-active (FeL_6^{3+} dissolved in L does not react with $Fe(X\text{-}phen)_3^{2+}$).

In the evaluation of the β parameters we started with estimates obtained from treating the variation of n_{tmp} with $[Fe(III)]_T$ given from the NMR data. The values were then optimized by fitting the kinetics data (Fig. 3) to Eq. (9a) where the rate constants are composite constants valid for the particular ionic strength and counterion concentration present. In the fitting procedure the free *tmp* concentration was supplied from the roots of the material balance equation through Newton's method,

$$[L]^5 + [L]^4\{\beta_1 - [L]_0\} + [L]^3\{\beta_2 - \beta_1([L]_0 + Fe(III)]_T)\} - [L]^2\{\beta_3 - \beta_2([L]_0 + 2[Fe(III)]_T)\} + [L]\{\beta_4 - \beta_3([L]_0 + 3[Fe(III)]_T)\} - \beta_4([L]_0 + 4[Fe(III)]_T) = 0,$$

derived from the material balance equations, $[Fe(III)]_T = [FeL_6^{3+}] + [FeL_5^{3+}] + [FeL_4^{3+}] + [FeL_3^{3+}] + [FeL_2^{3+}]$, and $[L] - [L]_0 = [FeL_5^{3+}] + 2[FeL_4^{3+}] + 3[FeL_3^{3+}] + 4[FeL_2^{3+}]$. For both the *phen* and 5,6-Me_2*phen* systems the FeL_5^{3+} path is not important.

The β values that account for both the kinetics (Fig. 4) and the NMR data (Table 2) are listed in Table 3. The [*tmp*] dependence measured at high salt concentration could be described with the same set of β-values (inset of Fig. 4). Therefore the solvation equilibria can be considered as unaffected by salt, relative to the effect of salt on the redox rate constants.

Evaluation of Ion Pairing Equilibria

The reaction of each Fe^{3+} species is considered as varying with both the ionic strength and the counterion concentration. Both effects are accounted for by the reaction model proposed in the preceding paper [2]. Summarized, all iron(III) solvate species, denoted as Fe^{3+}, form (species-invariant) mono and bis perchlorate ion pairs,

$$Fe^{3+} + ClO_4^- \Leftrightarrow Fe(ClO_4)^{2+} \quad K_1 \tag{5}$$

$$Fe(ClO_4)^{2+} + ClO_4^- \Leftrightarrow Fe(ClO_4)_2^+ \quad K_2 \tag{6}$$

Slight ion pairing is also allowed for the ferroin reactant,

$$Fe(Xphen)_3^{2+} + ClO_4^- \Leftrightarrow Fe(Xphen)_3(ClO_4)^+ \quad K_3 \tag{7}$$

The value for K_3 is known [2], and we assume that it is the same for all *phen* complexes used.

Thus, six concurrent reaction paths for each Fe^{3+} species are considered, shown in Eq. (8a–f).

$$\left.\begin{aligned} Fe^{3+} + Fe(Xphen)_3^{2+} &\longrightarrow \\ Fe(ClO_4)^{2+} + Fe(Xphen)_3^{2+} &\longrightarrow \\ Fe^{3+} + Fe(Xphen)_3(ClO_4)^+ &\longrightarrow \\ Fe(ClO_4)^{2+} + Fe(Xphen)_3(ClO_4)^+ &\longrightarrow \\ Fe(ClO_4)_2^+ + Fe(Xphen)_3^{2+} &\longrightarrow \\ Fe(ClO_4)_2^+ + Fe(Xphen)_3(ClO_4)^+ &\longrightarrow \end{aligned}\right\} \text{products} \qquad \begin{aligned} &(8a)\\ &(8b)\\ &(8c)\\ &(8d)\\ &(8e)\\ &(8f) \end{aligned}$$

In addition, each reaction path is taken as ionic strength dependent through electrostatic work required to bring the positively charged species together. The approximation was made that the increase in rate through ion-pairing is due to lowering the electrostatic work needed to bring the reactants together.

The resulting expression for the pseudo-first-order rate constant for the case that all solvation equilibria are rapid is given by Eq. (9),

$$k_{obsd} = Q\frac{(\beta_4 k_2 + \beta_3 k_3[L] + \beta_2 k_4[L]^2 + \beta_1 k_5[L]^3)[\text{Fe(III)}]_T}{([L]^4 + \beta_1[L]^3 + \beta_2[L]^2 + \beta_3[L] + \beta_4)} \tag{9a}$$

where

$$Q = \frac{(e^{6A}) + K_1[X](e^{4A}) + K_3[X](e^{3A}) + K_1K_3[X]^2(e^{2A})}{(1 + K_3[X])(1 + K_1[X] + K_1K_2[X]^2)} + \frac{K_1K_2[X]^2(e^{2A}) + K_1K_2K_3[X]^3(e^A)}{(1 + K_3[X])(1 + K_1[X] + K_1K_2[X]^2)} \tag{9b}$$

and [1, 5]

$$A = \frac{7.12(I)^{1/2}}{1 + 0.48\,r(I)^{1/2}} - \frac{15}{r} \tag{9c}$$

where $[\text{Fe(III)}]_T$ is the total iron(III) concentration, taken in large excess, and $[X]$ is free $[ClO_4^-]$. Both the free perchlorate concentration and the ionic strength have been calculated as in [3]. Likewise, the approach distance (r) was taken as 14 Å as done there. The subscripts on the rate constants denote the number of *tmp* ligands bound. The first term in the numerator of Eq. (9b) corresponds to Eq. (8a), and so on. On the basis of Eq. (9c), the rate constants in Eq. (9a) refer to infinite ionic strength. It should be emphasized that this point of reference merely means that no electrostatic work is required to bring the charged reacting species together ("electrostatics free" rate constants) as would be the case in a fused salt [5, 6]. One, however, can easily convert these rate constants to any desired ionic strength by using Eq. (9).

In the previous report [2], observed rate constants of a similar system involving two reactive solvate species could not satisfactorily be fitted to an equation similar to Eq. (9) unless the assumption was introduced that the two solvate species react via different ion-paired paths. Thus, an appreciable improvement in the fits was attained when the less reactive species were allowed to be redox-active only in precursor complexes having at least two perchlorate ions attached. This means omitting the terms of e^{nA} ($n = 6$–3) in Eq. (9b) for that path (ionic scheme 3, see below). The rationalization is that the less reactive a solvate species, the more is the assistance of perchlorate ions needed for the redox reaction to proceed (see Conclusions). Figure 3 of the present study substantiates this view: the rate increase by salt is much larger at high *tmp* concentrations where less reactive ferric species are available.

In the analysis of the salt dependences of Fig. 3, the approximation was made that under each condition (low and high *tmp* level) two solvate species prevail. Thus Eq. (9) was reduced to Eq. (10) and applied to each salt dependence separately,

$$k_{obsd}F = Q_A k_A + Q_B k_B \tag{10}$$

where $k_{obsd}F$ is the normalized rate constant of Fig. 3, and k_A and k_B are fit parameters representing composite rate constants. For Q_A and Q_B, differently modified expressions of Eq. (9b) were employed until both curves were coherently fitted with the use of one set of ion-pairing equilibrium constants K_1 and K_2; Eq. (5–6). For this purpose a further ionic path had to be introduced (ionic scheme 1, see below) characterized by excluding ion triplets, though present, from reacting. Thus the following schemes are adopted:

Ionic scheme 1: The reaction proceeds only via paths 8a–d.
Ionic scheme 2: All pathways are utilized, 8a–f.
Ionic scheme 3: The reaction proceeds only via paths 8d–f.

Within this framework, the plots of Fig. 3 could be described very well (solid lines in the figure) upon the following assumptions. In the case of no extra *tmp* added, Q_A and Q_B correspond to ionic schemes 1 and 2, respectively. At high *tmp* level, on the other hand, ionic schemes 2 and 3 were applied instead. In this way, non-linear least squares fits to each data set yielded one value for $K_1 = 70\,M^{-1}$ and one for $K_2 = 15\,M^{-1}$ (Table 3). Both values seem quite reasonable numerically on the following basis.

Remember that in our model the association constants are approximated as real constants within the experimental ionic strength range. (They cannot be corrected to the infinite ionic strength reference point used since they approach zero by theory.) Thus, the ion-association constants above, calculated from the kinetic analysis, should agree with those derived from conductance measurements valid for unit activity and corrected to the experimental conditions of this work. This is the case in fact. Conductance data of 3:1 electrolyte perchlorates similar to our's in moderate dielectric solvents (*Me*CN, *dmso*, *dmf*) indicate ion-pairing constants $K_1{}^0$ for zero ionic strength on the order of several hundreds, say 500–1000 M^{-1} [7, 8]. These reduce to some value of below one hundred for millimolar ionic strength on

the basis of Eq. (11),

$$K_1 = K_1{}^0 \exp \frac{7.12(I)^{1/2}}{1 + 0.48\, r(I)^{1/2}} \tag{11}$$

which is written for *Me*CN; cf. Eq. (9c). Further, for ion tripling, values of K_1 and K_2 are often taken to be linked by the Fuoss ratio [8, 9],

$$K_1/K_2 = \exp\left[560.75/(D_S r)\right] \tag{12}$$

where D_S is the static dielectric constant and r is the distance parameter in Å. Our value equal to $70/15 = 4.7$ is predicted by Eq. (12) if $r = 10$ Å.

Evaluation of Second-order Rate Constants

The non-linear $\log A/t$ plots indicate a solvation equilibrium that is no longer established rapidly compared to the redox reaction. Since the formation rates of solvate species might be related to solvation thermodynamics [10], the β-values from Table 3 would suggest that the formation equilibria of both $FeL_2{}^{3+}$ and $FeL_3{}^{3+}$ are slow. A species diagram (Fig. 5) indicates that peak concentrations of these complexes are built up at low total iron(III) concentrations. (Note that the concentration of $FeL_2{}^{3+}$ is *increased* upon dilution as occurring in the stopped-flow experiments.) However, neither greatly exceeds the ferroin reactant concentration which is 0.1 mM throughout.

Therefore, it can be concluded that during the first-order range found in the early stages (Fig. 1B) of the fast *Me*$_4$*phen* and *Me*$_6$*phen* reactions, $FeL_2{}^{3+}$ and $FeL_3{}^{3+}$ are maintained at steady state concentrations. In the late stages when the redox reaction is slowing down, the solvate species accumulate towards the equilibrium

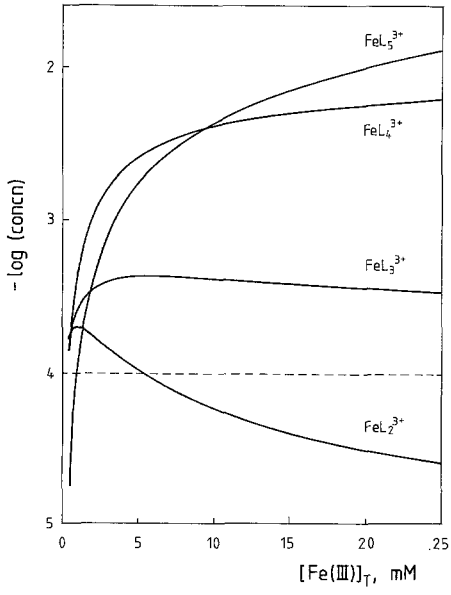

Fig. 5. Plots of $-\log$ of the concentrations of the reactive species present in solution within the relevant Fe(III) concentration range, derived from the β-values from Table 3. The broken line represents the ferroin concentration used in all experiments

values and rates are increased. If, however, the redox process is speeded up by the addition of salt (as in Fig. 1C), the slow equilibria lag behind.

Thus, for all systems, two limiting cases can be envisaged. For the initial stages, both FeL_2^{3+} and FeL_3^{3+} are non-equilibrium species whose concentrations are just half of the drive syringe solutions, with the equilibria of FeL_4^{3+} and FeL_5^{3+} established, giving the initial limiting rate constant $k(i)_{lim}$. For the final stages, all species are equilibrated, giving $k(e)_{lim}$. Since each kinetics experiment can be assumed to take place somewhere between these two extreme cases depending on the individual condition, it should always be valid that $k(i)_{lim} \lesssim k(i)_{obsd}$ and $k(e)_{lim} \gtrsim k(e)_{obsd}$. Further, $k(e)_{lim}$ should equal k_{obsd} that is the pseudo-first-order rate constant obtained from experiments having extra *tmp* added. Values of $k(e)_{obsd}$ were obtained, only as a guide, from the slopes of the non-linear semilogarithmic plots taken between the fourth and the fifth half live such as is shown in Fig. 1A.

For the evaluation of second-order electron-transfer rate constants, Eq. (9) was applied in the form of Eq. (13),

$$k_{lim} = Q_2k_2[FeL_2^{3+}] + Q_3k_3[FeL_3^{3+}] + Q_4k_4[FeL_4^{3+}] + Q_5k_5[FeL_5^{3+}]. \quad (13)$$

In this analysis, all of the 5–6 experimental series performed for each reaction system have been treated simultaneously, using the equilibrium parameter values from Table 3. With these, all species concentrations for both limiting cases as well as the free perchlorate concentrations were calculated. (The equilibrium concentrations of FeL_4^{3+} and FeL_5^{3+} have been calculated from the material balance equations, $[Fe(III)]_T - ([FeL_2^{3+}]_0 + [FeL_3^{3+}]_0) = [FeL_6^{3+}] + [FeL_5^{3+}] + [FeL_4^{3+}]$, and $[L] - [L]_0 = [FeL_5^{3+}] + 2[FeL_4^{3+}] + 3[FeL_3^{3+}]_0 + 4[FeL_2^{3+}]_0$, where $[FeL_2^{3+}]_0$ and $[FeL_3^{3+}]_0$ are given as half of the concentrations of the drive syringe solutions.)

With all concentrations for each experimental condition thus given, second-order rate constants were adjusted so that for any data point the conditions (i) k_{obsd} (pseudo-first-order) $= k(e)_{lim}$, (ii) $k(i)_{lim} < k(i)_{obsd}$, and (iii) $k(e)_{lim} > k(e)_{obsd}$ were fulfilled. In most instances this aim could be achieved. In the procedure, we selected one data point from the pseudo-first-order range where equilibrium conditions are clearly valid, as reference point. For that point the rate constants k_2 to k_5 were computed by means of a linear transformation method when the reactivity ratios and the ionic schemes for each species were supplied. Preliminary values for the reactivity ratios were derived from fits of Eq. (9) to the experimental data for the high *tmp* concentration (i.e. pseudo-first-order) range. With the rate constants thus obtained, values for $k(i)_{lim}$ and $k(e)_{lim}$ were calculated for all data points. Now the reactivity ratios were set equal to a variety of values until for any data point the above-mentioned conditions were fulfilled.

Table 4 has tabulated the complete 5,6-Me_2phen case for an illustration. All the other experimental and calculated kinetics data are given as supplementary material. Table 5 reports the rate constants and also gives the ionic schemes that were assigned to each solvate species in accordance with the analysis of Fig. 3. These rate constants reveal a reactivity-selectivity relationship (RSR) as is displayed in Fig. 6. Another representation is given by the inset of Fig. 6 which has arbitrarily chosen the rate constants of the 4,7-Me_2phen system as a parameter. The common point of intersection in both plots occurs at the rate constant equal to about $2 \times 10^8\ M^{-1}\,s^{-1}$. This rate constant is predicted for the oxidation of a $Fe(Xphen)_3^{2+}$

Table 4. Kinetics data for the Fe(III) oxidation of Fe(5,6-$Me_2phen)_3^{2+}$ at various conditions (25 °C)

$[tmp]_0$ mM	$[S]_T$[a] mM	$[Fe(III)]_T$ mM	$k(i)_{lim}$ s^{-1}	$k(i)_{obsd}$ s^{-1}	$k(e)_{obsd}$ s^{-1}	$k(e)_{lim}$ s^{-1}
[tmp]-Variation						
0	0	10	3.17	4.40	7.10	7.80
2	0	10	2.81	3.90	6.10	6.42
4	0	10	2.50	3.10	4.90	5.34
6	0	10	2.23	2.60	3.80	4.49
8	0	10	2.00	2.40	3.30	3.81
10	0	10	1.80	2.20	2.80	3.26
12	0	10	1.62	1.80	2.50	2.81
14	0	10	1.47	1.50	2.33	2.44
16	0	10	1.33	1.35	2.00	2.13
18	0	10	1.21	1.30	1.70	1.88
20	0	10	1.11	1.23	1.40	1.66
25	0	10	0.89	1.00	1.10	1.25
30	0	10	0.72	0.90	0.90	0.97
40	0	10	0.50	0.62	0.62[b]	0.62
50	0	10	0.36	0.45	0.45	0.42
60	0	10	0.27	0.31	0.31	0.32
80	0	10	0.16	0.19	0.19	0.18
100	0	10	0.10	0.12	0.13	0.12
150	0	10	0.05	0.06	0.06	0.05
200	0	10	0.02	0.03	0.03	0.03
$[Bu_4NClO_4]$-*Variation at high [tmp]*						
200	0	10	0.028	0.027	0.027	0.028
200	20	10	0.051	0.044	0.044	0.052
200	40	10	0.073	0.060	0.060	0.073
200	60	10	0.092	0.077	0.077	0.093
200	80	10	0.108	0.087	0.087	0.109
200	100	10	0.123	0.101	0.101	0.124
200	120	10	0.135	0.117	0.117	0.136
200	140	10	0.146	0.134	0.134	0.147
200	160	10	0.156	0.148	0.148	0.157
200	180	10	0.165	0.148	0.148	0.165
200	200	10	0.172	0.172	0.172	0.173
$[Bu_4NClO_4]$-*Variation*						
0	0	2	1.76	2.60	3.30	4.43
0	20	2	4.96	7.50	11.3	11.7
0	40	2	7.04	10.2	15.4	15.9
0	60	2	8.40	11.4	16.7	18.4
0	66	2	8.71	12.0	17.0	18.9
0	80	2	9.31	13.6	19.1	19.9
0	100	2	9.96	14.5	20.5	20.9
0	120	2	10.4	15.4	20.7	21.5
0	140	2	10.8	16.0	21.0	21.9
0	160	2	11.0	16.7	21.9	22.2
0	180	2	11.2	17.0	22.0	22.4
0	200	2	11.4	17.6	21.9	22.5

Table 4. (*Continued*)

Table 4. *(Continued)*

$[tmp]_0$ mM	$[S]_T$[a] mM	$[Fe(III)]_T$ mM	$k(i)_{lim}$ s^{-1}	$k(i)_{obsd}$ s^{-1}	$k(e)_{obsd}$ s^{-1}	$k(e)_{lim}$ s^{-1}
[Fe(III)]-*Variation without added* Bu_4NClO_4						
0	0	1	1.26	1.47	2.20	2.76
0	0	2	1.76	1.75	2.92	4.43
0	0	3	2.05	2.11	3.20	5.42
0	0	4	2.27	2.45	4.42	6.07
0	0	5	2.45	2.44	4.91	6.53
0	0	7	2.76	2.92	5.60	7.17
0	0	10	3.17	3.41	6.30	7.80
0	0	12	3.43	3.67	6.90	8.13
0	0	14	3.67	3.81	7.50	8.41
0	0	16	3.91	3.94	8.00	8.67
0	0	20	4.36	4.48	8.63	9.13
0	0	24	4.78	5.08	9.00	9.55
[Fe(III)]-*Variation at constant* $[ClO_4^-]$						
0	69	1	9.54	10.7	15.4	18.6
0	63	3	8.03	9.40	14.8	18.0
0	57	5	7.17	8.24	14.2	16.2
0	51	7	6.64	7.31	12.8	14.7
0	45	9	6.27	7.15	12.6	13.7
0	33	13	5.74	6.25	11.0	12.1
0	27	15	5.52	5.91	10.6	11.5
0	21	17	5.33	5.90	9.80	10.9
0	12	20	5.08	5.65	9.46	10.3
0	0	24	4.79	5.35	9.00	9.55

[a] $S = Bu_4NClO_4$

[b] Reference point, see text

complex with reduction potential equal to 0.9 V (vs. BCr, Table 1) independent of the Fe(III) speciation. Noteworthy, the rate constants for the reductions of $Fe(dmf)_3(MeCN)_3^{3+}$ and $Fe(dmf)_4(MeCN)_2^{3+}$ by $Fe(Me_6phen)_3^{2+}$ and $Fe(Me_4phen)_3^{2+}$, respectively, from the previous report [2] fit in the picture of Fig. 6.

Although the rate constants cannot be given with the desired precision, we strongly believe that the RSR is real and would not get lost in the noise level of some sort of error analysis. It may be remembered that >60 data points were used for each system comprising rate constants that vary by more than 2 orders of magnitude but nevertheless had to fulfill the conditions described above. As judged from varying the reactivity ratios and comparing observed and calculated limiting rate constants, the uncertainty of the resulting second-order rate constants may be in the range about 20%. However, the operation of the RSR, usually a domain of organic chemistry [11–14], is readily obvious by inspecting the most instructive experimental series that is the rate constant dependence on Fe(III) reactant at constant perchlorate level (Fig. 2), where counterion and ionic strength effects are minimized. If the relative reactivities of the solvate species were invariant with

Table 5. Overall ionic paths[a] and rate constants ($M^{-1}s^{-1}$) with no electrostatic work for the redox reactions of the various solvate species and ferroin complexes

Iron(II) complex of	FeL_2^{3+}	FeL_3^{3+}	FeL_4^{3+}	FeL_5^{3+}
Me_6phen	1 3.6×10^6	2 7.2×10^5	3 6.0×10^4	3 2.9×10^3
Me_4phen	1 1.8×10^6	2 2.6×10^5	3 2.1×10^4	3 9.3×10^2
4,7-*Me_2phen*	1 1.5×10^6	2 1.5×10^5	3 8.2×10^3	3 2.3×10^2
5,6-*Me_2phen*	1 6.7×10^5	2 4.8×10^4	3 1.7×10^3	
phen	1 4.3×10^5	2 2.1×10^4	3 4.3×10^2	

[a] Indicated by the numbers above the rate constants and described in the text

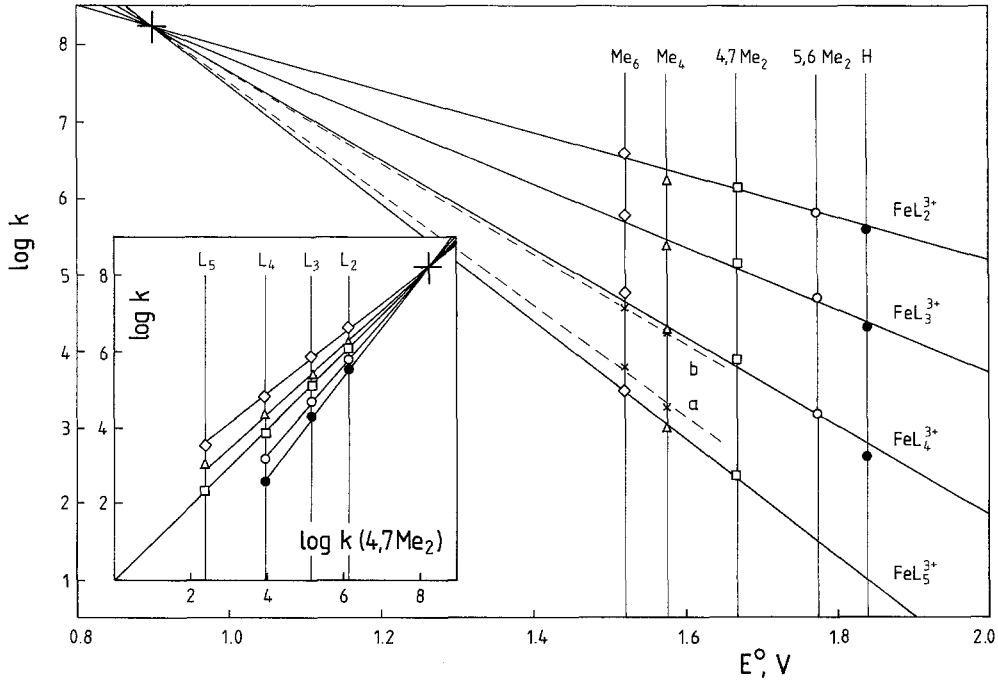

Fig. 6. Electrostatics free second order rate constants for the oxidation of the various solvate species as a function of the reduction potential of $Fe(Xphen)_3^{3+/2+}$ with substituents X indicated. The broken circles refer to the rate constants of the reductions of $Fe(dmf)_3^{3+}$ and $Fe(dmf)_4^{3+}$ given in the previous work [2]. Inset.: LFER with the rate constants of the $Fe(4,7\text{-}Me_2phen)_3^{2+}$ reaction chosen as a parameter

$Fe(Xphen)_3^{2+}$, one trend in the rate constants should be observed. Instead there is a shift of the maximum in going from $Fe(phen)_3^{2+}$ to $Fe(Me_6phen)_3^{2+}$. (In the case of phen and 5,6-Me_2phen, the maximum is outside the experimental concentration range.) This feature reflects the increasing importance of the FeL_4^{3+} and eventually the FeL_5^{3+} paths in the more reactive systems (cf the species diagram in Fig. 5). Given the many simplifying assumptions made, the agreement between observed and calculated trends for the initial rate constants is generally reasonable as shown in Fig. 2.

The occurrence of the RSR would indicate that the inner-shell reorganization energy is not only part of the exponential term of the rate equation but is also included in the pre-exponent. An increasing number of recent papers indeed present the pre-exponent as a function of the activation barrier [15].

Conclusions

The reaction systems dealt with turned out to be rather complex virtually reaching the limit of adequate analysis. Although the numerical values of the rate constants could not be defined with the desired precision, the more qualitative features are well-worth of consideration.

The results of using $Fe(tmp)_6^{3+}$ in place of $Fe(dmf)_6^{3+}$ are partly as expected. The weaker base *tmp* affects both the substitution and the redox behavior of iron(III): (i) *tmp* coordinated at Fe^{3+} is more easily replaced by *Me*CN, (ii) *tmp* stabilizes trivalent iron to a less extent [4], and (iii) the complexes containing *tmp* are more reactive (by one order of magnitude) towards reduction compared to the *dmf* analogues. Beyond that, however, the significant increase in reaction complexity is remarkable upon changing the ligand donor strength by a small margin. This is mainly the consequence of the fact that the reduction rates are more strongly affected in going from *dmf* to *tmp* than are the interconversion rates (ligand exchange).

An important result of the present work is connected with the salt dependences displayed in Fig. 3, contributing to the knowledge of the effect of ion pairing on electron transfer reactions. Thus, our earlier suggestion regarding similar systems previously studied [2] is substantiated that the various solvate species react via different ion-paired paths. This pattern obviously originates from the interplay of two factors, (1) the concurrent existence of several reacting species highly different in reactivity together with (2) the high charge-type of each reaction bringing about large electrostatic work terms. In order to elucidate the present situation it is useful to express the rate constant as (for the low-driving force case, i.e., omitting the quadratic term) [5, 16],

$$k = A \exp\left[-(w + \Delta G_{is}^{*} + \Delta G_{0s}^{*} + 0.5\,\Delta G^{0})/RT\right] \tag{14}$$

where the symbols have their usual meanings given in [5]. What is of primary interest here is the driving force ΔG^0 and the Coulombic work w needed to bring the reactants together. As seen from Table 1, there is a mean reduction potential difference of 0.20 V for the replacement of one *tmp* by *Me*CN. This makes the driving force between two solvate species in the series differ by 19 kJ. Further, the work required for precursor complex formation in acetonitrile may be calculated by the use of the quantity A in Eq. (9c) [5],

$$w = -Z_1 Z_2 ART. \tag{15}$$

Thus, for the $+2/+3$ reaction (path 8a), for an arbitrary ionic strength of 5 mM Fe(III) without extra added salt, w is about 7.5 kJ. This value reduces to 2.5 kJ if Fe^{3+} reacts as the triplet, i.e., for the $+/+2$ charge-type of path 8e. The resulting difference in Coulombic work of 5 kJ when Fe^{3+} reacts as such or as the triplet is half of the value of $0.5\,\Delta G^0$. Therefore, the overall reactivity of e.g. FeL_3^{3+} tends to be roughly comparable to that of $FeL_4X_2^{+}$. In sum, the lower the driving force of a species the more counterions are needed for competition with the next species of higher driving force in the series.

On the other hand the pathway for the most reactive species, FeL_2^{3+}, the driving force is so high that precursor complex stability appears to be of minor importance. The fact that ion triplets, though presumably present, were not needed in the analysis could well mean that the presence of two perchlorates in the precursor makes electron transfer less likely [6, 17]. Further work will show whether the matter described is of more general validity.

Supplementary Material

Further experimental and calculated limiting initial and final rate constants for the various *phen* complexes under various conditions have been deposited and can be obtained from the author (8 pages).

Acknowledgements

This work was supported by the Fonds zur Förderung der wissenschaftlichen Forschung in Österreich (Project Nos. 5548 and 8126). Also, thanks go to Prof. John P. Hunt (Washington State University, Washington, USA) for making possible the NMR measurements.

References

[1] Schmid R., Kirchner K., Dickert F. L. (1988) Inorg. Chem. **27**: 1530
[2] Schmid R., Kirchner K., Sapunov V. N. (1989) Inorg. Chem. **28**: 4167
[3] Schmid R. (1983) J. Solution Chem. **12**: 135
[4] Kirchner K., Jedlicka R., Schmid R. (1992) Monats. Chem. **123**: 203
[5] Schmid R. (1991) Revs. Inorg. Chem. **11**: 255
[6] Jedlicka R., Kirchner K., Schmid R. (in press) J. Chem. Soc. Dalton Trans.
[7] Braga T. G., Wahl A. C. (1985) J. Phys. Chem. **89**: 5822
[8] Pethybridge A. D. (1982) Z. Phys. Chem. (Munich) **133**: 143
[9] Iwamoto E., Monya S., Yamamoto Y. (1983) J. Chem. Soc. Faraday Trans. 1 **79**: 625
[10] Emmenegger F. P. (1989) Inorg. Chem. **28**: 2210
[11] Huisgen R. (1970) Angew. Chem. Int. Ed. Engl. **9**: 751
[12] Exner O., Giese B. (1978) Angew. Chem. Int. Ed. Engl. **17**: 775
[13] Giese B. (1984) Acc. Chem. Res. **17**: 438
[14] Linert W., Sapunov V. N. (1988) Chem. Phys. **119**: 265
[15] (a) Sutin N. (1983) Progr. Inorg. Chem. **30**: 441. (b) Weaver M., Gennet T. (1985) Chem. Phys. Lett. **113**: 213. (c) Marcus R. A., Sumi H. (1986) J. Chem. Phys. **84**: 4894. (d) Grampp G., Harrer W., Jaenicke W. (1987) J. Chem. Soc., Faraday Trans. 1 **83**: 161
[16] Nielson R. M., Wherland S. (1984) Inorg. Chem. **23**: 1338
[17] Anderson K. A., Wherland S. (1991) Inorg. Chem. **30**: 624

Received July 17, 1992. Accepted November 25, 1992